Mapping of forest species and tree density using new Earth Observation sensors for wildfire applications

Iphigenia Keramitsoglou[*a], Charalambos Kontoes[b], Konstantinos Koutroumbas[b], Olga Sykioti[b], Nicolaos Sifakis[b]

[a]University of Athens, Department of Applied Physics, Remote Sensing and Image Processing Team, Panepistimioupolis, Build. PHYS-V, GR-15784, Athens, Greece.

[b]Institute for Space Applications and Remote Sensing, National Observatory of Athens, Metaxa & Vas. Pavlou St, Pendeli, Athens, GR-15236, Greece

ABSTRACT

The success of any decision support system for managing wildfires lies on its ability to simulate fire evolution. Therefore, accurate information on the natural fuel material in any area of interest is necessary. The present study aims to provide methodological tools to explore in depth the potential of new Earth Observation data for horizontal mapping of vegetated areas. Two approaches are mainly described. The first one deals with the classification of ASTER visible, near- and short-wave infrared images in a detailed nomenclature including both different species and tree densities. This is important for wildfire studies since the same vegetation classes may represent completely different risk ignition levels depending on their morphological characteristics (i.e., trees height and density). The improvement of class separability using hyperspectral images acquired by Hyperion is also investigated. The second approach refers to a pattern recognition software tool for single tree counting using a very high spatial resolution image acquired by IKONOS-2 satellite. According to this approach, the regions dense in plants are identified by applying a suitable thresholding on the image. The resulted regions are further processed in order to estimate the number and location of single trees based on a pre-specified crown size per stratified zone. The outcome of the latter approach may provide direct evidence of tree density relating to ground biomass. Finally, the two approaches are used in a complementary manner to explore the possibilities offered by new sensor technology to override past limitations in species and fuel classification due to inadequate spectral/spatial resolution. The pilot application area is Mount. Pendeli and the east side of Mount. Parnitha, in the prefecture of Attiki, Greece.

Keywords: biomass; classification; forest fire; tree counting

1. INTRODUCTION

Forest fire incidents are known to provoke irreparable damage to regions of utmost significance from the ecological point of view. The development of operational systems for managing such incidents is of great significance for both the authorities and end-users. The success of such a system strongly depends on the performance of the forest fire simulation tool for operational needs that would estimate the way fire evolves. In order to develop an efficient and complete mathematical model for fire spread behavior and fire perimeter growth, a curve growth formulation as well as a reliable expression for correlating fire spread over the factors influencing it such as terrain slope, vegetation growth and density and current meteorological conditions are needed[1-3].

The aim of the work is to provide fire modelers with a reliable and valid assessment of vegetation cover types and fuel maps taking into consideration canopy structure and biomass spectral properties. For that reason, we exploit the potential of Earth Observation (EO) data provided from state-of-the-art sensors, in combination with in-situ observations, to develop a standardized method to assess forest ecosystem vegetation parameters. Three different types

[*] ikeram@phys.uoa.gr; phone: +30-210- 727 6843; fax: +30-210- 727 6774

Remote Sensing for Agriculture, Ecosystems, and Hydrology VII, edited by Manfred Owe, Guido D'Urso, Proc. of SPIE Vol. 5976, 59760G, (2005) · 0277-786X/05/$15 · doi: 10.1117/12.626600

of EO images are used in the study, namely (i) multispectral High Spatial Resolution ASTER (Advanced Spaceborne Thermal Emission and Reflection Radiometer) images; (ii) hyperspectral Hyperion images; and (iii)multispectral Very High Spatial Resolution IKONOS-2 images.

ASTER is an advanced multispectral imager that was launched on board NASA's Terra spacecraft in December, 1999. ASTER covers a wide spectral region with 14 bands from the visible to the thermal infrared (TIR) with high spatial, spectral and radiometric resolution. It consists of three separate subsystems, each operating in a different spectral region, using separate optical systems. These subsystems are the VNIR (Visible and Near InfraRed), the SWIR (ShortWave InfraRed) and the TIR. The spatial resolution varies with spectral region: 15 m in the VNIR, 30 m in the SWIR and 90 m in the TIR. The major innovative features of ASTER are: (i) simultaneous earth surface images from the visible to the thermal infrared; (ii) higher geometric and radiometric resolution in each band than current satellite sensors, (iii) near infrared stereoscopic image pairs collected during the same orbit, (iv) exquisite optics that allow the instrument axis to move as much as ± 24 degrees for SWIR and TIR cross-talk direction from the nadir, and (v) highly reliable cryocoolers for the SWIR and TIR sensors[4].

The VNIR high resolution radiometer observes the targets using solar radiation reflected from the earth surfaces in three visible and near infrared bands useful primarily for land survey, vegetation assessment, environmental protection and disaster prevention. On the other hand, SWIR is an advanced high resolution multispectral radiometer which detects reflected solar radiation from the earth surfaces in the wavelength region of 1.6 – 2.43 micrometer. SWIR is especially advantageous for resources discrimination such as rocks and minerals and for environmental survey such as vegetation types and volcanoes.

The hyperspectral Hyperion sensor, onboard EO-1 (launched in November 2000), has a 16-day repeat cycle and acquires data in pushbroom mode with two spectrometers, one in the visible and near infrared (VNIR) range and another in the short-wave infrared (SWIR) range. Hyperion provides continuous spectral coverage over 220 bands collected with a complete spectrum with high radiometric accuracy, with a ground sample distance (GSD) of 30 meters for all bands. Each Hyperion scene is collected as a narrow strip, covering a ground area of approximately 7.7 km in the across-track direction, and 42 km or 185 km in the along-track direction (depending on the original data acquisition request; http://eo1.usgs.gov/userGuide/hyp_prop.html)

Moreover, the launch and subsequent acquisitions of the IKONOS platform in 1999 have heralded a new era by providing very high spatial resolution images. IKONOS-2 satellite is on a sun-synchronous low earth orbit at a nominal altitude of 681 km and has a revisiting capability of 3 days. The sensor's instantaneous field of view is such that it collects images of the Earth with a very high spatial resolution of 1 and 4m in the panchromatic and multispectral modes, respectively. The four IKONOS-2 multispectral channels are tuned to detect radiation in the visible spectrum (450–530nm centered in the blue, 520–610 nm centered in the green and 640–720nm in the red) as well as in the near infrared spectrum (770–880 nm). At these resolutions, ecologists are able to directly identify certain species (e.g. detection of individual tree crowns) and species assemblages[5]. Due to the higher costs of these images, IKONOS-2 images were used only for fine scale forest mapping, where detail is considered more crucial.

The present pilot application takes place in the mountain area of Penteli and the east side of Mount. Parnitha in the prefecture of Attika in Greece. The selection of this area is of great interest because it is one of the mountain areas mostly hit by fires in Greece. It is located north-northeast of the city of Athens; on its slopes there are a lot of built up areas. In the Penteli area, there have been many conflagrations registered with detrimental effects such as loss of human lives, forests, properties, and homes. It is remarkable that on June 13, 1992 a fire burned 241 km^2. Penteli is covered with vegetation, which consists of the most flammable forest species such as *Aleppo pine* (high forest and reforestation), and *holm oak*. Mount Parnitha on the other hand has an extended area of *fir* trees.

The ultimate goal of the present study is to provide methodological tools to explore in depth the potential of new EO data for horizontal mapping of vegetated areas. For that purpose, *we explore the potential of image synergistic interpretation through the integration of complementary data (in VNIR & SWIR) in order to obtain more information than cannot be derived from single sensor data alone.* Two approaches are mainly described: (i) classification of multispectral ASTER complementary data (in VNIR and SWIR) and hyperspectral Hyperion images and (ii) pattern recognition for single tree counting using an IKONOS-2 image.

2. METHODOLOGY

The work undertaken can be divided in two main approaches, namely (i) classification of multispectral ASTER complementary data (in VNIR and SWIR) and hyperspectral Hyperion images and (ii) pattern recognition for single tree counting using an IKONOS-2 image. These are described next.

2.1 Classification

2.1.1. Classification of ASTER complementary data

ASTER products AST2B05V and AST2B05S (i.e. surface reflectance in VNIR and SWIR) acquired at two different dates are used. The first acquisition was in autumn (13/10/2003) and the second one in the following spring (21/03/2004).

First, all images are resampled to 25m. In order to generate a new image containing the information present in the available satellite images, these are geometrically corrected and georeferenced with the highest possible precision. For this purpose we use a 2nd degree polynomial transformation with Ground Control Points (GCP). In theory, six GCPs are enough in order calculate the parameters of this polynomial, however we identify 14 GCP uniformly distributed in the image. The success of transformation is checked by means of the mean square error which in this case is 7 m, that is to say roughly one third of a pixel (25m).

The second step of the pre-processing deals with the exclusion of correlated spectral bands from further processing. Five bands from each image are kept as non correlated. Following that, a *new image* is generated with the ten selected bands from both dates. This is illustrated in Table 1.

Layer of new image	ASTER Band	Date of acquisition
1	1 VNIR	13/10/2003
2	2 VNIR	13/10/2003
3	3 VNIR	13/10/2003
4	1 SWIR	13/10/2003
5	5 SWIR	13/10/2003
6	1 VNIR	21/03/2004
7	2 VNIR	21/03/2004
8	3 VNIR	21/03/2004
9	1 SWIR	21/03/2004
10	5 SWIR	21/03/2004

Table 1: Layers of information of new image

The objective is to classify the study area using a *detailed nomenclature representing both tree species and densities*. For that reason, the area is divided in three “strata” (zones) by means of CORINE Land Cover 2000 database. These are:

(i) Forest,
(ii) Natural Vegetation, and
(iii) Transitional Forest.

There is also a fourth stratum of artificial surfaces but it is masked out. Representative sampling sections of approximately 1 km^2 were defined for each stratum. An experienced forester conducted the collection of in-situ data, by means of polygons with detailed description within each sampling section. These polygons are essentially the training samples. 5-10% of these samples are separated to be used as evaluation points for the assessment of the classification.

The remaining training samples are digitized, checked thoroughly and modified accordingly to ensure homogeneity within the polygons, before a number of tests is applied. The tests included:

- ellipses separability in feature space;
- transformed divergence[6]; and
- contingency matrix.

The basic approach followed is that the classification nomenclature is as detailed as possible. However, in cases where classes cannot be separated (according to the above mentioned tests), these are merged and named appropriately. The classification was performed using the (parametric) maximum likelihood algorithm taking into consideration the contingency matrix, together with the mean and standard deviation of the training samples . This resulted in a two-layer image (first and second guess). Following that, a fuzzy convolution was applied using a 3x3 kernel. The fuzzy convolution operation creates a single classification layer by calculating the total weighted inverse distance of all the classes in a window of pixels. Then, it assigns the center pixel in the class with the largest total inverse distance summed over the entire set of fuzzy classification layers. This has the effect of creating a context-based classification to reduce the speckle or salt and pepper in the classification[7].

2.1.2. Classification of Hyperion image

A single Hyperion scene acquired on September 20, 2004 covering an area of 7.6 x 86 km^2 was processed.

Due to a large number of stripped bands not all bands were usable. Therefore the following procedure was applied in order to reduce the initial number to 63 bands, preserving as much as possible the spectral information.

Step 1. Create separate files for Visible, NIR and SWIR bands.
Step 2. Removal of bands presenting dense striping.
Step 3. Calculation of Principal Components Analysis (PCA) for each spectral area.
Step 4. Location of remaining non systematic stripes detected in the secondary PCA components
Step 5. Creation of a new subset with the reduced bands.
Step 6. Recalculation of PCA for the remaining bands.
Step 7. Return to Step 4 until stripping is random and located to small areas.
Step 8. Computation of the correlation matrix for each file.
Step 9. Selection of the less correlated bands.
Step 10. Creation of a new file with the 63 remaining bands.

After band reduction, the scene was reduced to an area 7.6m wide and 25km long, focused on Mt. Parnitha. The image was then resampled to 25m resolution and geometrically corrected to the Hellenic reference system (EGSA87). Atmospheric corrections were not applied since humidity measurements in the area one hour before, one hour after and during the image acquisition did not show levels of relative humidity high enough (i.e., >70%) that could significantly influence the spectral signature (average relative humidity was measured to be 50%).

Classification was then performed using the method of maximum likelihood feature space fuzzy classification without non-parametric rule and two best classes per pixel. It was performed separately on two major strata, “Forest” and “Transitional Forest-Natural Vegetation”. The Transitional Forest and Natural Vegetation strata were unified due to the small area covered by the latter.

2.2. Single tree counting on IKONOS-2 image

The proposed method makes assessments of the position and the crown size of the single tree within a forested area using as input very high spatial resolution imagery derived by satellite sensor or airborne acquisitions. The imagery used can be panchromatic or color, the latter being the result of the fusion of panchromatic with multispectral data, with a spatial resolution of 1m (e.g. IKONOS) or higher (0.5m-0.8/pixel, aerial photography, Quickbird, etc). The proposed method is implemented through the employment of a specifically developed algorithm based on combinations of low level image processing, segmentation and pattern recognition techniques. The algorithm’s current level of development allows the treatment of B&W imagery or respectively the 1st Principal Component of a multi-channeled image, which also forms a B&W image layer. Pixel data of either 8 or 16 bits per pixel can be used as input to the algorithm.

The basic principle dominating the algorithm's development is the need to be applicable not only within fields where trees are normally distributed and well separated from one another (e.g. fields of tree cultures or agricultural olive farms), but also within dense forested areas, where crowns of a tree stand are connected or overlap each other and significant tree crown information is hidden due to shadows caused from neighboring trees or relief. To overcome these difficulties, the algorithm is designed to be supervised by the analyst, the latter entering auxiliary knowledge relating to the mean tree crown size per segment area, denoted as *cr*, and the expected tree crown overlap $d_{overlap}$. For this the proposed method makes use of an additional layer of information introducing polygons, hereinafter denoted as regions, representing the tree vegetation classes found in the area of interest, associating for each vegetation class the expected values for the parameters *cr* and $d_{overlap}$. This layer can be any existing vegetation layer of the area of interest or it can be the output of a common tree species classification problem, using high resolution satellite imagery (ASTER) as it is the case in this study. The proposed method considers each region of the whole area separately and tries to identify objects through their shadows. Specifically, for each region all of its (disconnected) sub-regions are identified. For each sub-region X the following actions take place.

Step 1 ***Histogram equalization.*** The minimum, x_{min}, and the maximum, x_{max}, values of the pixels contained in X are identified and the value of each pixel x is transformed to $y = \frac{x - x_{\min}}{x_{\max} - x_{\min}} 255$, resulting to a new contrast stretched image of X, denoted by X_c.

Step 2 ***Thresholding.*** On the intensity histogram $h(x)$ of X_c, the position x_t where $\sum_{x=0}^{x_t} h(x) = t_1$ is identified where t_1 is an a priori defined parameter. Let X_t be the resulting image.

Step 3 ***Identification of objects*** (disconnected regions) in X takes place by utilizing X_t.

Step 4 ***Elimination of objects*** whose number of pixels is less than a predefined threshold.

For each object Y in X the following actions are carried out:

- ***Computation of the area***, $A(Y)$, of Y (=number of pixels of Y).
- ***Determination and refinement of the boundary*** $B(Y)$ of Y.
- ***Computation of a circularity index.*** This index shows how close to circularity is Y[1]. It is defined as

$$C(Y) = \frac{\sum_{x \in B(Y)} | d(x, x_m) - \bar{d} |}{|B(Y)|}, \quad (1)$$

  where x_m is the mean of $B(Y)$ and, $\bar{d} = \frac{\sum_{x \in B(Y)} d(x, x_m)}{|B(Y)|}$, is the mean distance of the pixels on the boundary of Y from its center and $|B(Y)|$ is the number of points on $B(Y)$. As the formula in (1) shows, the smaller the values of $C(Y)$ the higher the degree of circularity.
- If $A(Y)$ is less than a predefined threshold A_0[2] or is less than a predefined threshold A_1 and exhibits high circularity[3] then:

[1] This is important for example in the case where the object that exhibits high circularity and its area is comparable to the mean tree crown size for the corresponding region. Then it is likely that the object corresponds to an isolated tree.
[2] A_0 is of comparable size with the mean tree crown size of the corresponding region.
[3] A_1 equals a few times A_0 (typically 3-5 times). Also, the high circularity is expressed by the condition $C(Y)<1$.

- Estimate a single tree centered at the mean of Y (as it is computed taking into account only its boundary pixels).

- Else if A(Y) is greater than A_1 or A(Y) is less than A_1 but it exhibits low circularity[4] (this is a strong indication that we have an agglomeration of trees) then the following actions are carried out

  - ***Histogram equalization*** on *Y* (as in the general case)**.** Let Y_c be the result of this action.

  - ***Thresholding*** on Y_c (where the threshold is set equal to 50). Let Y_t be the thresholding result.

  - ***Identification of objects*** (disconnected regions) in *Y* takes place by utilizing Y_t.

  - ***Elimination of objects*** whose number of pixels is less than a predefined threshold (typically, this threshold equals to a few pixels).

  - Estimation of the number of trees, *k*, that belong to *Y*, as $\frac{A(Y)}{cr * d_{overlap}}$, where $d_{overlap}$ as mentioned is the index measuring the expected degree of overlap among the trees. The higher the value of $d_{overlap}$, the less the degree of overlap among the trees is.

  - If *k* equals *1* then

    - Estimate a single tree centered at the mean of *Y*.

  - Else if *k* is greater than *1*, then

    - Perform the *BSAS* clustering algorithm[8] for estimating initial positions for the trees in the area.
    - Perform the *k-means* algorithm for refining the previous result and to distribute the estimated positions of the trees more evenly in the *Y* area.

The algorithm is tested on a very high spatial resolution panchromatic IKONOS image representing the main forested zones of the Penteli mountain. The spatial resolution of the image layer used is of 1m. The tree species classification map derived from the use of ASTER image data acquired over the same area, is used as additional layer to supervise the algorithm's output as described in the beginning of this section.

3. RESULTS

3.1. Image Classification

The classified image for each stratum was evaluated by means of:

1. overall performance;
2. confusion matrix[9];
3. kappa statistics; and
4. photo-interpretation.

The following table summarizes the results of all classification experiments. It should be stressed that the area covered by ASTER image is 625 km^2 whereas by Hyperion is 190 km^2.

[4] Low circularity is expressed by the condition *C(Y)>1*.

Sensor	Stratum	Number of classes	Overall performance	Overall Kappa statistics
ASTER	Forest (F)	21	84%	0.71
	Natural Vegetation (NV)	9	84%	0.76
	Transitional Forest (FT)	19	79%	0.76
Hyperion	Forest (F)	10	90%	0.89
	Transitional Forest – Natural Vegetation (FT-NV)	10	94%	0.93

Table 2: Overall classification results for ASTER and Hyperion sensors

Classification accuracy of Hyperion image is assessed using the method of "equalised random reference pixels", which allows lessening the bias in the results, due to lack of adequate number of ground-truth polygons in the limited area covered by Hyperion scene. For ASTER complementary data, the assessment was performed using a subset of the ground-truth data acquired during the field survey. The overall accuracy results for both classification experiments are presented in Table 2. The accuracy of ASTER products as well as the number of identified classes is dependent on the strata. The overall accuracy of the classified maps varies from 79-84% and of kappa coefficient from 0.71-0.76. The output of Hyperion classification seems to be less dependent on the strata and more accurate than ASTER (overall accuracy from 90 to 94%; kappa coefficient from 0.89 to 0.93). The number of identified classes can not be directly compared between Hyperion and ASTER map, as the areas covered are different.

In terms of species and densities separability the results are presented in Tables 3 and 4.

HYPERION	Strata			
	Forest		Transitional Forest- Natural Vegetation	
Species	*Identified*	*Densities*	*Identified*	*Densities*
Aleppo pine	X	3	X	3
Fir	X	2	X	1 (unified)
Coppice	X	3	X	2
Evergreen broad leaved	X	1	X	2
Grasslands	-	-	X	1
Bare soil	X	1	X	1

Table 3: Vegetation species identified and classified in each stratum (X) using the Hyperion image. The number of classes representing different densities discriminated for each vegetation species is given.

ASTER	Strata					
	Forest		Natural Vegetation		Transitional forest	
Species	*Identified*	*Densities*	*Identified*	*Densities*	*Identified*	*Densities*
Black pine	X	1	-	-	-	-
Fir	X	2	-	-	X	1
Broad leaved deciduous	X	1	-	-	-	-
Deciduous oak	X	1	-	-	-	-
Aleppo pine	X	1 (unified)	-	-	X	1 (unified)
Shrub	X	1	-	-	-	-
Coppice	X	4	X	3	X	3
Evergreen broad leaved	X	3	X	1 (unified)	X	3
Maquis	X	1	X	2	X	4
Grasslands	X	4	X	1	X	1
Natural regeneration of forest	-	-	-	-	X	3

Table 4: Vegetation species identified and classified in each stratum (X) using the ASTER images. The number of classes representing different densities discriminated for each vegetation species is given.

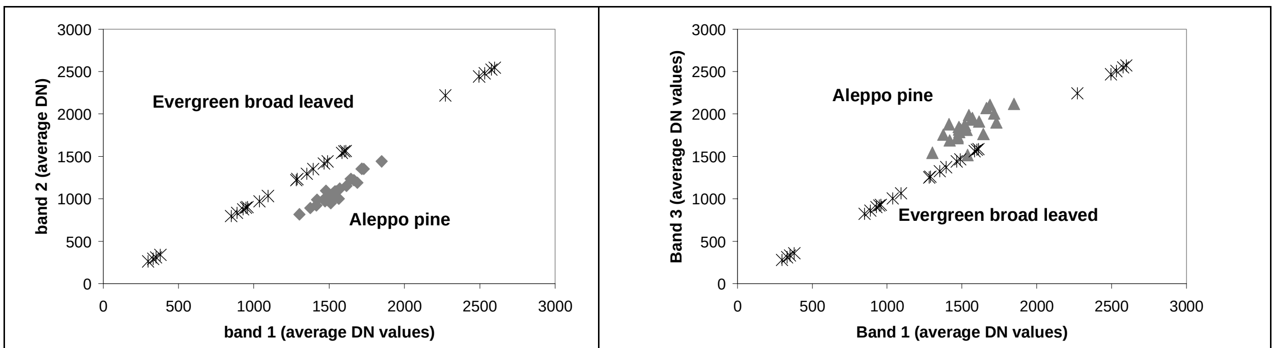

(a) **(b)**

Figure 1: Average DN values for samples of evergreen broad leaved and Aleppo pines in a two dimensional feature space of Hyperion data. The average DN values are calculated from the Hyperion bands that cover the corresponding ASTER band.

The classification showed that the area acquired by Hyperion is essentially covered by *aleppo pine* and *evergreen broad leaved forest*. In elevations that exceed 500 meters *fir forest* predominates as expected. Table 3 shows that in the stratum Forest, three different densities of *aleppo pine* are discriminated, two for *firs*, three for *coppice* and one for *evergreen broad leaved trees*. In strata Transitional Forest and Natural Vegetation, three densities of *aleppo pine* are discriminated. For the *fir* category differentiation in density was not possible. Moreover, two densities of *coppice* are distinguished, two in *evergreen broad leaved trees* and one in grasslands. The equivalent results from the classification of ASTER images are presented in Table 4. In this case the identified species are more than the ones of the Hyperion, however this can be attributed to the larger area covered by ASTER- it is more than triple the size. It is interesting to compare the two Tables and note that *aleppo pine* which is a predominant species of the area can be better discriminated into different density classes using Hyperion rather than ASTER images. For the latter, although there are enough training polygons provided, it is impossible to detect the different densities, therefore there appears to be one class (unified) which includes all density levels. The opposite is true for *evergreen broad leaved forest*, i.e. three density levels were discriminated in F and FT strata using ASTER images. *Coppice* densities are distinguished effectively both with ASTER and Hyperion data.

In terms of species classification a satisfactory separability is observed between the different classes. Coniferous (*aleppo pines* and *firs*) and *evergreen broad leaved trees* present distinct spectral signatures and are differentiated without difficulty (Table 3 and 4). It is the same in the case of the other classes (grasslands, coppice and bare soil). On the other hand, *aleppo pines* and *firs*, both belonging in the coniferous category, were difficult to distinguish with Hyperion data, and this was, to a large degree, imposed by the training polygons.

Figure 1 shows the average DN values for samples of two main vegetation classes in the area (*evergreen broad leaved* and a*leppo pines*) in a two dimensional feature space of Hyperion data. The average DN values are calculated from the Hyperion bands that cover the corresponding ASTER band. ASTER band 1 corresponds to Hyperion bands 18-25. Band 2 corresponds to 30-34 Hyperion bands. ASTER band 3 corresponds to 45-52 Hyperion bands. The graphs show that the two species present adequate separability.

3.2. Tree counting

Figure 2 shows a detail of the derived map of points representing the location of trees overlaid on the original IKONOS image.

The tree counting algorithm results are compared against the outcome of several independent human photo-interpretations. The photo-interpreters digitized tree positions in specifically defined test areas, which represent all types of vegetation and tree densities, found in the area of interest. Algorithm underestimations and overestimations in tree counting are identified and measured per test area in respect to the photo-interpretation results. This error analysis shows that in the totality of the test areas, the total number of trees counted by the algorithm is deviating from the one given by photo-interpretation by only 5%. Indeed in a total of 3332 trees counted by photo-interpretation the algorithm identified a number of 153 trees less. By considering tree underestimations and overestimations separately without adding them at test area level, it is concluded that the error level associated to the current version of the algorithm and image data used is of the order of 25%. Even this result is not far of being acceptable and the method being considered operational, given that the algorithm enables the identification of locations of trees and crowns for a total of 25770 trees in less than 4 hours of machine processing. This should require several days of human interpretation to derive.

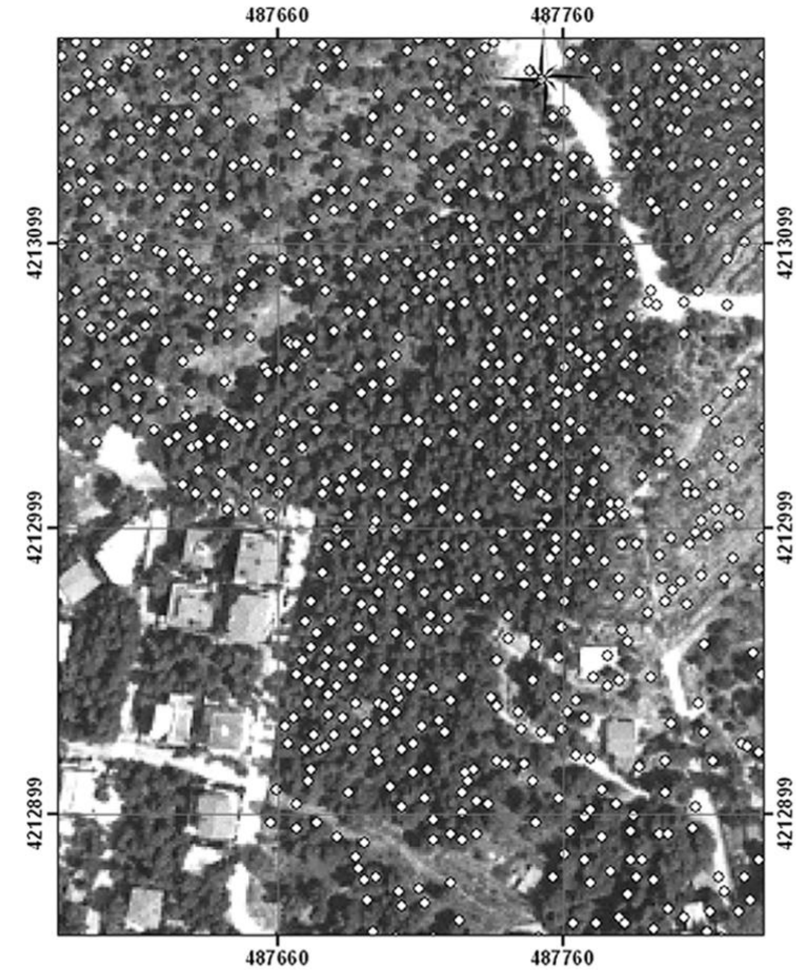

Figure 2: The derived tree locations overlaid on the original IKONOS image (coordinates are in meters)

4. CONCLUDING REMARKS

The aim of the present study is to explore the feasibility of classification and pattern recognition software tools on new Earth Observation data for horizontal mapping of vegetated areas. Two approaches are mainly described. The first one deals with the classification of ASTER visible, near- and short-wave infrared images and Hyperion hyperspectral images in a detailed nomenclature including both different species and tree densities. This is important for wildfire studies since the same vegetation classes may represent completely different risk ignition levels depending on their morphological characteristics (i.e., trees height and density). Although direct comparison is difficult to perform as the scene covered by Hyperion is only a subscene of ASTER, some general conclusions can be drawn based on the work carried out.

Both ASTER and Hyperion images have comparable spatial resolution, which indicates that the working scale for vegetation mapping is fundamentally the same. However, the ASTER swath is larger than the Hyperion's making the area covered by a single scene of the latter sensor much limited (7.6 km). In terms of spectral characteristics, Hyperion is considered superior, as the 242 bands (out of which 63 are used here) with approximately 10nm width offer multiple layers of information. However, two points need to be stressed: one is that these bands often contain *correlated signals* (see Figure 1), and the other is that *Hyperion does not provide bands in the thermal infrared*. Nevertheless, the latter is not an issue here, as thermal information is not used in any of the classification experiments. The superiority of spectral information is reflected on the results of the classification of Hyperion image (see Table 2) which exceeds 90%. The ability to discriminate individual species and densities depends on the stratum and the species itself, as the detailed confusion matrices indicate. Finally, the cost of ASTER images is 0.02 € per km^2 whereas it varies from 9 to 36 € per km^2 for Hyperion images.

Based on the above, a generic conclusion is that ASTER images are cheaper to achieve, easier to process and cover a larger area in a single scene providing an adequate working and mapping scale and added-value classification maps of acceptable accuracy. However, at local level, if additional information or superior thematic accuracy is needed, one can use Hyperion images in a complementary manner to increase the classification accuracy and class discrimination provided by ASTER.

As far as the tree counting algorithm is concerned which provides detailed information at local level, at the moment it is tested on very high spatial resolution imagery (digital orthophotos of 0.5m spatial resolution) and on colored satellite and aerial digital imagery of similar spatial resolution (0.5-1m). The first results are very encouraging. However, these will be further evaluated and presented in the frame of a comparative study examining the role of parameters relating to spatial resolution, number of input layers (panchromatic, coloured, PCA), tree species, data radiometric resolution. This analysis is expected to be the content of another publication in near future.

Acknowledgements

The work presented in this paper is funded by the Operational Programme "Competitiveness", Action 4.5.1, Project Code: 4. ASTER images were provided in the framework of ASTER ARO AP-232 contract awarded by Earth Remote Sensing Analysis Data Center.

References

1. Keramitsoglou I., C.T. Kiranoudis, H. Sarimveis, N. Sifakis, A multidisciplinary decision support system for forest fire crisis management, Environmental Management, 33 (2): 212-225, 2004.
2. Vakalis D, Sarimveis H, Kiranoudis CT, Alexandridis A, Bafas G, A GIS based operational system for wildland fire crisis management I. Mathematical modelling and simulation, Applied Mathematical Modelling, Vol 28, pp 389-410, 2004.
3. Vakalis D, Sarimveis H, Kiranoudis CT, Alexandridis A, Bafas G, A GIS based operational system for wildland fire crisis management II. System architecture and case studies, Applied Mathematical Modelling, Vol 28, pp 411-425, 2004.
4. ASTER User's Guide, Part I, Ver. 3.1., ERSDAC Earth Remote Sensing Analysis Center, March 2001.
5. Turner, W., Spector., Gardiner., Fladeland, M., Sterling and Steininger. M., Remote sensing for biodiversity science and conservation. Trends in Ecology and Evolution, Vol. 18, pp 306-314, 2003
6. Jensen, J. R., Introductory Digital Image Processing: A Remote Sensing Perspective. 2nd edition, Englewood Cliffs, New Jersey: Prentice-Hall, 1996.
7. ERDAS, Leica Geosystems: ERDAS Field Guide, 7th edition. GIS & Mapping, LLC Atlanta, Georgia, 2004.
8. Theodoridis S., and K. Koutroumbas, Pattern Recognition, 2nd edition, Academic Press, 2003.
9. Congalton R., A Review of Assessing the Accuracy of Classifications of Remotely Sensed Data, Remote Sensing of Environment, Vol. 37, pp 35-46, 1991.